

ISPH Numerical Modeling of Nonlinear Wave Run-up on Steep Slopes

Memarzadeh, Rasoul^{1*}; Hejazi, Kourosh²

1- Dept. of Engineering, Shahid Bahonar University of Kerman, Kerman, IR Iran

2- Dept. of Civil Engineering, K.N.Toosi University of Technology, Tehran, IR Iran

Received: May 2012

Accepted: October 2012

© 2012 Journal of the Persian Gulf. All rights reserved.

Abstract

Non-breaking tsunami waves run-up on steep slopes can cause severe damages to coastal structures. The estimation of the wave run-up rate caused by tsunami waves are important to understand the performance and safety issues of the breakwater in practice. In this paper, an Incompressible Smoothed Particle Hydrodynamics method (ISPH) method was utilized for the 2DV numerical modeling of nonlinear wave run-up on steep slopes. SPH is a meshless method based on particles, which is capable of high accurate modeling of free surface flows with large deformations. In developed model, mass and momentum conservation equations were solved in a Lagrangian form using a two-step fractional method. In the first step, Navier-Stokes equations were solved to compute velocity components by omitting pressure term and in the absence of incompressible condition. In the second step, the continuity constraint was satisfied and the resulting Poisson equation was solved to calculate pressure terms. Velocity values were then corrected and surface positions were computed. In the present model, a new technique was applied to allocate density to the particles for the calculations. By employing this technique, ISPH model was stabilized. The developed ISPH model was first validated by the solitary wave propagation on the constant water depth and the corresponding results showed good agreement with analytical results. The convergence of the method and the sensitivity of relevant model parameters were discussed. Then, validated model was used to study the run-up of solitary waves on steep slopes by considering a coastal breakwater for various wall steepnesses (i.e. 1:1, 2:1, 4:1, 8:1 and vertical wall).

Keywords: *ISPH, Fractional step method, Nonlinear wave, Solitary wave, Steep slopes, Run-up.*

1. Introduction

Tsunamis can propagate shoreward, where they undergo changes induced by the near-shore topography and increase in height. These waves can propagate shoreward and damage coastal structures. The estimation of the wave run-up rate is important

to understand the performance and safety issues of the breakwater in practice. Solitary wave or combinations of solitary-like waves are often used to simulate the run-up and shoreward inundation. The first investigation on the run-up of solitary waves was the laboratory study of Hall and Watts (1953). They used a rectangular channel with a plane beach and established a relationship between dimensionless

* Email: rasoul.memarzadeh@eng.uk.ac.ir

wave height a/d , the beach slope and the dimensionless run-up R/d of the form:

$$R/d = k(\beta)(a/d)^{\phi(\beta)} \quad (1)$$

Where K and Φ were reported to be functions of the beach angle β . This result was later confirmed in the experimental studies of Camfield and Street (1969) and Saeki et al. (1971). Synolakis (1986) experimentally studied some physical processes of run-up of breaking and non-breaking solitary waves to understand some coastal effects of tsunamis. Hsiao et al. (2008) presented new laboratory experiments of solitary wave evolution on a 1:60 plane beach and used measured data to re-examine existing formulae that included breaking criterion, amplitude evolution and run-up height. They proposed a simple formula which could predict maximum run-up height for a breaking solitary wave on a uniform beach with a wide range of beach slope (1:15–1:60).

Since then, equation (1) has been used extensively to check numerical calculations. The first attempt to find a numerical solution to the problem of solitary wave propagation over constant depth, and then climbing a sloping beach was made by Heinter and Housner (1970). They solved the shallow water wave equations including a term to correct for friction by using the finite element method. They presented some surface profiles for propagation and run-up of solitary waves and infinite bores and reported good agreement with the experimental data on maximum run-up. Kim et al. (1983) used a boundary integral method to solve the equations of motion for the problem of a run-up of a solitary wave generated by a piston movement in a numerical wave tank. They presented data for maximum run-up of solitary waves and reported good agreement with the Hall and Watts (1953) data. Zelt (1991) modeled the run-up of nonbreaking and breaking solitary waves on plane impermeable beaches with a Lagrangian finite-element, Boussinesq wave model. For the steep slope, he considered only waves which did not break on run-up, and obtained excellent agreement with the laboratory data. Lo and Shao (2002)

developed an incompressible smoothed particle hydrodynamics (SPH) method together with a large eddy simulation (LES) to simulate the near-shore solitary wave mechanics. They solved the Navier–Stokes equations in Lagrangian form using a two-step fractional method. They simulated cases of a solitary wave against a vertical wall and running up a plane slope by their model and presented good agreement with the wave profiles and reported experimental data or analytical solutions. Wood et al. (2003) used a Navier–Stokes solver to examine steep waves as they run-up a steep beach. They used the volume of fluid method (VOF) to model the free surface. Fuhrman and Madsen (2008) considered the numerical simulation of nonlinear wave run-up within a highly accurate Boussinesq-type model.

According to this literature, numerical methods have become an important tool for simulating these problems. In general, to model water waves, numerical methods can be classified into four approaches. These approaches are grid-based methods (e.g. Finite Volume Method), methods combining a grid with particles (e.g. Marker-and-Cell method), methods combining a grid with a surface finder, which use a fixed grid to solve the PDE's governing fluid motion (e.g. Volume-of-Fluid method), and particle methods, without grid (e.g. Smoothed Particles Hydrodynamics method).

The marker and cell (Harlow and Welch., 1965) and volume of fluid (Hirt and Nichols, 1981) methods are two of the most flexible and powerful models for simulating such flows, in which the Navier–Stokes equations were solved on a fixed Eulerian grid. In MAC method marker particles used to define the free surface while in VOF method governing equations were solved for the volume fraction of the fluid.

The two most popular particle methods are Smoothed Particle Hydrodynamics (SPH) and Moving Particles Semi-implicit (MPS). SPH originally developed for astrophysical computations (Lucy, 1977 and Monaghan, 1992) and was later extended to model a wide range of fluid mechanic problems (Monaghan,

1994). As there is no mesh distortion, the SPH method can efficiently treat the large deformation of free surfaces and multi interfaces. SPH simulations of the incompressible flows could be performed by two methods: 1) approximately simulating incompressible flows with a small compressibility, namely Weakly Compressible SPH (WCSPH); 2) simulating flows by enforcing incompressibility, namely Incompressible SPH (ISPH). In WCSPH method, the flow was considered as slightly compressible, with a state equation for the pressure calculation (Monaghan, 1994). In ISPH method, the pressure-velocity coupling is generally achieved by the projection method (Chorin, 1968; Cummins and Rudman, 1999).

SPH method has been shown to be applicable to a wide range of problems. A summary is presented in Table 1.

Table 1. Illustrative list of different applications of SPH method for fluid mechanic problems

Description of the work	Used Model	Authors
Wave propagation	WCSPH	Monaghan and Kos (1999)
Gravity currents	WCSPH	Monaghan (1996)
Free surface Newtonian and non-Newtonian flows	ISPH	Shao and Lo (2003)
Wave interactions with porous media	ISPH	Shao (2010)

In the following sections, the details of the ISPH model developed for the water waves and some modifications for standard ISPH method including applying a new technique to allocate density of the particles for the calculations, are presented. At first, the developed model was validated by the solitary wave propagation on the constant water depth and the corresponding results showed good agreement with analytical results.

A simple analysis of the convergence and accuracy of the numerical scheme was made and the convergence rate of the numerical model and the sensitivity of relevant parameters were quantified. Then, by using the validated model, the run-up of solitary wave on steep slopes was simulated and breakwater steepness effect on the run-up of solitary wave by considering a coastal breakwater for various

wall steepnesses were studied.

2. ISPH Numerical Model

2.1. Governing Equations

The governing equations of viscous free surface flows contain mass conservation and momentum conservation equations, as follows (Shao and Lo., 2003):

$$\frac{1}{\rho} \frac{D\rho}{Dt} + \nabla \cdot \mathbf{u} = 0 \quad (2)$$

$$\frac{D\mathbf{u}}{Dt} = -\frac{1}{\rho} \nabla p + \frac{\mu}{\rho} \nabla^2 \mathbf{u} + \mathbf{g} \quad (3)$$

Where ρ is the density, \mathbf{u} is the velocity vector, P is the pressure and \mathbf{g} is the gravitational acceleration.

2.2. Two Steps Fractional Algorithm

After defining initial conditions of problem, such as geometry of problem, smoothing distance, number of particles, mass, initial coordinate and velocity of them, computations were implemented with two steps fractional algorithm.

In the standard ISPH method, density of particles like other initial conditions, such as their mass was defined before the start of computational time steps. In the present model, a new technique was applied to allocate density of the particles for the calculations, which in beginning of each time step density of particles was defined using equation (4) and implemented in computations.

$$\rho_i^0 = \sum_j m_j \widehat{W}(|r_i - r_j|, h) \quad (4)$$

Afterwards, the computations of the ISPH method began in two basic steps (Shao and Lo., 2003). In the first step, Navier-Stokes equations were solved to compute velocity components by omitting pressure term and in the absence of incompressible condition. In the second step, the continuity constraint was satisfied and the resulting Poisson equation was solved to calculate pressure terms. ISPH method could be summarized in a simple algorithm

combined of four steps (Shao and Lo., 2003):

1. The prediction step: Compute forces by considering gravitational and viscosity term in Eq. (3). Apply them to particles and find temporary particle positions and velocities.

$$\Delta \bar{u}_* = (\bar{g} + \frac{\mu}{\rho} \nabla^2 \bar{u}) \Delta t \quad (5)$$

$$\bar{u}_* = \bar{u}_t + \Delta \bar{u}_* \quad (6)$$

$$\bar{r}_* = \bar{r}_t + \bar{u}_* \Delta t \quad (7)$$

Where \bar{u}_t and \bar{r}_t are particle velocity and position at time t , \bar{u}_* and \bar{r}_* are temporary particle velocity and position, respectively and $\Delta \bar{u}_*$ is change in the particle velocity during the prediction step. Incompressibility was not satisfied in this step and the fluid density that was calculated based on the temporary particle positions (ρ_i^*) deviates from the initial density of particles (ρ_i^0).

$$\rho_i^* = \sum_j m_j \bar{W}(|r_i^* - r_j^*|, h) \quad (8)$$

2. The correction step; in this step the pressure term, obtained from the mass conservation Eq. (3), was used to enforce incompressibility in the calculation.

$$\frac{1}{\rho_0} \frac{\rho_0 - \rho_*}{\Delta t} + \nabla \cdot (\Delta \bar{u}_{**}) = 0 \quad (9)$$

$$\Delta \bar{u}_{**} = \frac{-1}{\rho_*} \nabla P_{t+1} \Delta t \quad (10)$$

By combining equations (9) and (10) Poisson equation obtained which by solving it pressure of particles defined.

$$\nabla \cdot \left(\frac{1}{\rho_*} \nabla P_{t+1} \right) = \frac{\rho_0 - \rho_*}{\rho_0 \Delta t^2} \quad (11)$$

After employing the relevant SPH formulation for the Laplacian operator, a system of linear equations was obtained and solved efficiently by iterative solvers.

3. New particle velocities were computed by equations (10) and (12).

$$\bar{u}_{t+1} = \bar{u}_t + \Delta \bar{u}_{**} \quad (12)$$

4. The new position of particles was obtained by Eq. (12).

$$\bar{r}_{t+1} = \bar{r}_t + \frac{\bar{u}_{t+1} + \bar{u}_t}{2} \Delta t \quad (13)$$

2.3. SPH Principles

In a SPH computation, the fluid was discretized into an assembly of individual particles and the SPH formulation was obtained as a result of interpolation between them. The interpolation was based on the theory of integral interpolants that uses kernel function to approximate delta function. All the terms in the governing equations were treated by using the particle interaction models and thus the grid was not required. A detailed explanation of the SPH theories could be found in (Monaghan, 1992). The kernel approximation of f was written in the form:

$$f(r) = \int_{\Omega} f(r) \bar{W}(|r-r_0|, h) dr \quad (14)$$

in the particle approximation, for any function of field variable:

$$f(r_i) = \sum_j \frac{m_j}{\rho_j} f(r_j) \bar{W}(|r_i - r_j|, h) \quad (15)$$

Where, Ω is support domain, m_j and ρ_j are the mass and density of particle j , m_j/ρ_j is the volume element associated with particle j , \bar{W} is interpolation kernel (in this paper, kernel based on the spline function was used (Monaghan, 1994)), r is position vector, h is smoothing distance which determines width of kernel and ultimately the resolution of the method and in this paper $h = 1.2 \times dr$ were used, where dr is the initial particle spacing, and n the total number of particles within the smoothing length that affects particle i .

The gradient term in the Navier–Stokes equation can have different forms in SPH formulation. Monaghan (1994) proposed a model of gradient that conserves linear and angular momentum:

$$\frac{1}{\rho_i} (\nabla P_i) = \sum_j m_j \left(\frac{P_j}{\rho_j^2} + \frac{P_i}{\rho_i^2} \right) \cdot \nabla_i \bar{W}_{ij} \quad (16)$$

Where P is pressure of particles.

The Laplacian for the pressure and viscosity term was formulated as the hybrid of a standard SPH first derivative coupled with a finite difference approximation for the first derivative (Shao and Lo., 2003). The purpose was to ensure the numerical stability, as the second

derivative of SPH kernels was very sensitive to the particle disorder. Thus, developing a model of Laplacian that prevents this instability was very important. These are represented by:

$$\nabla \cdot \left(\frac{1}{\rho} \nabla P \right)_i = \sum_j m_j \frac{8}{(\rho_i + \rho_j)^2} \frac{P_{ij} \vec{r}_{ij} \cdot \nabla_i \tilde{W}_{ij}}{|\vec{r}_{ij}|^2 + \eta^2} \quad (17)$$

$$\left(\frac{1}{\rho} \nabla \cdot \vec{\tau} \right)_i = \left(\frac{\mu}{\rho} \nabla^2 \vec{u} \right)_i = \sum_j \frac{4m_j (\mu_i + \mu_j) \vec{r}_{ij} \cdot \nabla_i \tilde{W}_{ij}}{(\rho_i + \rho_j)^2 (|\vec{r}_{ij}|^2 + \eta^2)} (\vec{u}_i - \vec{u}_j) \quad (18)$$

Where $P_{ij} = P_i - P_j$, $\vec{r}_{ij} = \vec{r}_i - \vec{r}_j$, μ is the viscosity coefficient and η is a small number introduced to keep the denominator non-zero during computational and usually equal to $0.1h$. After employing the SPH formulation Eq. (17) for the Laplacian of pressure, the corresponding coefficient matrix of linear equations was symmetric and positive definite and can be efficiently solved by available solvers.

3. Free Surfaces and Wall Boundary Conditions

3.1. Free Surfaces

Since there were no particles in the outer region of free surface, the particle density decreases on this boundary. A particle which satisfied the following equation was considered to be on the free surface:

$$\rho_* < \beta \times \rho_0 \quad (19)$$

In this equation, β is the free surface parameter and $0.8 < \beta < 0.99$ (Ataie-Ashtiani et al., 2008). In this paper, $\beta = 0.97$ was used. Twice amount of Eq. (16) was applied for the free surface particles, in order to move correctly, avoid instability in computations and control over incompressibility condition for them (Ataie-Ashtiani et al., 2008).

3.2. Solid Walls

Solid walls were described by one line of particles. The velocities of wall particles were set zero to represent the non-slip boundary condition. In order to balance the pressure of inner fluid particles and prevent them from penetrating the solid walls, the pressure

Poisson equation was solved for these wall particles and the Neumann boundary condition was imposed. Also, in order to ensure that density of particles was computed accurately and wall particles were not considered as free surface particles, two lines of dummy particles placed outside of wall boundaries. The pressure of a dummy particle was set to that of a wall particle in the normal direction of the solid walls (Shao and Lo., 2003).

4. Convergence, Stability and Accuracy of Numerical Scheme

4.1. Convergence of ISPH Scheme

The individual fluid particles are discrete points and could deform as the real fluid does, so the number of the particles employed in the computation must be sufficiently large to achieve numerical convergence and realistic flow modeling. Until now, there were many analytical results available on the convergence criteria for the standard SPH method (Quinlan et al., 2006; Vaughan et al., 2008) and similar studies were also carried out for the ISPH method (Shao, 2010; Xu et al., 2009). In the following model verifications, the convergence of the ISPH approach were investigated by increasing the number of fluid particles into the computational domain until when the numerical results were close to either the theoretical or experimental values. Thus, the choice of particle spacing was a key factor for the numerical convergence.

4.2. Stability of ISPH Scheme

In the modeling of water flows, in which the fluid viscosity is not a control factor, the stability of the ISPH computation requires the following Courant condition to be observed:

$$\Delta t \leq 0.1 \frac{dr}{u_{\max}} \quad (20)$$

Where u_{\max} is maximum particle velocity in the computation. The factor 0.1 ensured that the particle

moved only a small fraction of the particle spacing per time step (Shao and Lo, 2003).

4.3. Accuracy of ISPH Scheme in Spatial Domain

The accuracy of the ISPH numerical scheme should be between $O(dr)$ and $O(dr^2)$ in the spatial domain. A simple theoretical analysis of the standard SPH algorithm has been made by Monaghan and Kos (1999). They proposed that the accuracy of second-order SPH integral interpolants was reduced when it was replaced by the summation interpolants in the SPH formulations. In developing the ISPH flow model, a first-order finite difference scheme was included in the Laplacian and viscosity equations (17) and (18). Thus, globally the spatial accuracy of ISPH scheme should be lower than the theoretical value of $O(dr^2)$. A quantified analysis of the model convergence rate will be investigated in the following section.

5. Results and Discussion

5.1. Model Verification-Solitary Wave Propagation on the Constant Water Depth

In this section, the accuracy of ISPH flow model was validated by comparing the numerical and theoretical wave heights of solitary wave propagation on the constant water depth. According to Lee and Raichlen (1982), the analytical solution for the wave profile and velocity derived from the Boussinesq equation:

$$\eta(x, t) = a \operatorname{sech}^2 \left[\sqrt{\frac{3a}{4d^3}} (x - ct) \right] \quad (21)$$

$$u = \eta \sqrt{\frac{g}{d}} \quad (22)$$

Where η is water surface elevation, a is wave amplitude, d is water depth, $c = \sqrt{g(d+a)}$ is wave celerity and t is time of propagation.

A solitary wave with the wave amplitude $a/d = 0.3$ was considered and the water depth $d = 0.2 \text{ m}$. To quantify the convergence behavior of the ISPH approach, two different spatial resolutions were used in the model tests, i.e. $dr = 0.01 \text{ m}$ and $dr = 0.02 \text{ m}$ to discretize a computational domain. Approximately 8,000 particles are involved in the computation with $dr = 0.01 \text{ m}$ and 2000 particles with $dr = 0.02 \text{ m}$. The initial arrangement of SPH particles follows that of Monaghan and Kos (1999): The SPH particles were placed on a regular grid with square cells, and those that were above the solitary wave profile were eliminated. This arrangement initially leads to a slightly jagged wave profile but the fluids rapidly adjust to a smoothed solitary wave. The fluid density ρ and kinematic viscosity ν were 1000 kg/m^3 and $10^{-6} \text{ m}^2/\text{s}$.

In Figure 1, the computed solitary wave profiles were compared with the analytical solution for $dr = 0.01 \text{ m}$ and two time steps involving $dt = 0.001 \text{ s}$ and $dt = 0.002 \text{ s}$ which satisfy Courant condition, i.e. Eq. 20. It was shown that the ISPH computations using $dt = 0.002 \text{ s}$, leading to the divergence of the numerical results and the ISPH computation using $dt = 0.001 \text{ s}$ demonstrates a satisfactory agreement with the analytical solution, however the computational costs would increase.

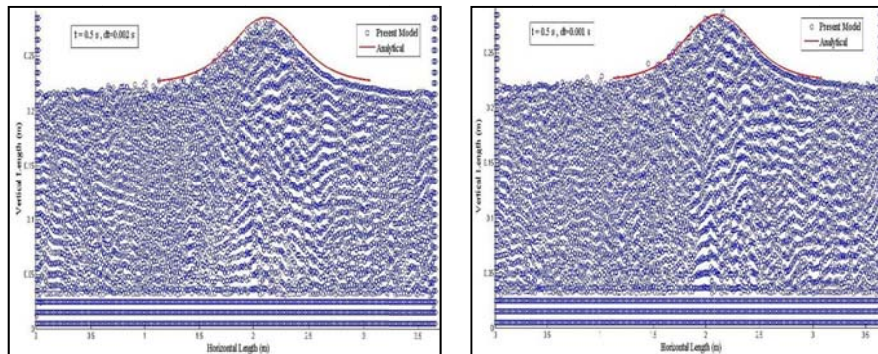


Fig. 1: Particle configurations and comparison of values computed by ISPH flow model and analytical surface profiles of solitary wave (horizontal and vertical scales units in meter)

In Figure 2, the computed solitary wave heights along propagation are compared with the analytical solutions. The computational results are presented using two different particle resolutions. From this figure, the maximum numerical error is 12.5% for the rough computation using $dr = 0.02\text{ m}$ and 5.7% for the refined computation using $dr = 0.01\text{ m}$ and it is obvious that the numerical results converged to the analytical solution as the particle size decreased or the particle number increased.

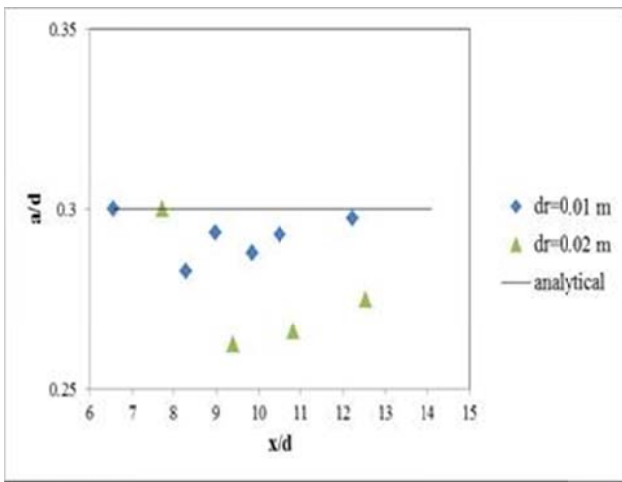


Fig. 2: Computed and theoretical solitary wave heights

To further quantify the convergence rate of the ISPH numerical scheme, the convergence analysis in Shao and Lo (2003) was used. It was assumed that the numerical error E_{dr} (by using a particle spacing of dr) with the analytical solution was proportional to dr^n , where n was the order of convergence. If $E_{0.02}$ and $E_{0.01}$ denote the numerical errors using a particle spacing of $dr = 0.02\text{ m}$ and 0.01 m , respectively, then the following relationship could be obtained:

$$\frac{E_{0.02}}{E_{0.01}} \approx \frac{(0.02)^n}{(0.01)^n} \quad (23)$$

$$\frac{E_{0.02}}{E_{0.01}} \approx 2^n$$

To determine value of n , differences in the wave height between the ISPH results and analytical solutions in Figure 2 were used. To calculate values of $E_{0.02}$ and $E_{0.01}$, the averaged numerical errors of model in computation solitary wave height during propagation is used. From the figure, values of $E_{0.02}$

and $E_{0.01}$, are 10.72% and 3%, respectively. Finally, using these values and Eq. (23), n or order of convergence was found around 1.8. Thus the ISPH numerical scheme for the free surface flows was concluded to be lower than second-order accurate at $O(dr^{1.8})$. This was consistent with the errors in the kernel functions being of second-order locally, and with the time integration and the formulation of the Laplacian reducing the order further.

5.2. Model Application-Non-breaking Solitary Wave Run-up

In the previous section, propagation of Solitary wave on the constant water depth was investigated. In this section, verified ISPH flow model was used to study a practical problem, i.e. run-up of non-breaking waves on a steep slope. These waves could propagate shoreward and damage coastal structures. The estimation of the wave run-up rate was important to understand the performance and safety issues of the breakwater in practice. The empirical formula (Hall and Watts, 1953) for solitary wave run-up on an impermeable slope with $\alpha = 45^\circ$ was used to verify the ISPH flow model computations for this problem:

$$\frac{R}{d} = 3.1\left(\frac{a}{d}\right)^{1.15} \quad (24)$$

Where R is wave run-up height, d the water depth and a the wave height. Then, the model was applied to study on solitary wave run-up on beaches with slopes 2:1, 4:1, 8:1 and vertical slope. In Figure 3, the initial conditions and geometry for this problem were shown.

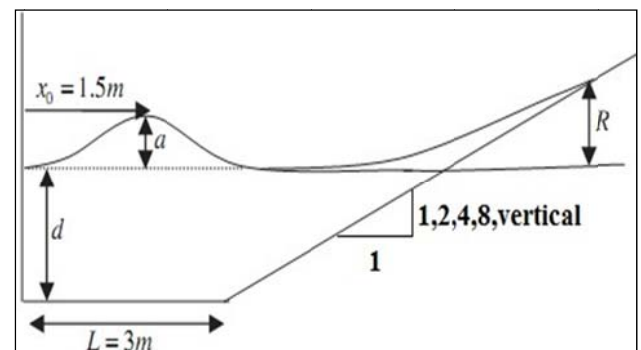


Fig 3: Geometry of Non-breaking solitary wave run-up

The initial particle spacing was 0.02 m for all of mentioned slopes and for each slope; problem was solved for two different cases of water depth and three wave amplitudes and for each, the run-up (R) was recorded. Details of used models are listed in Table 2. In this problem like the previous one, the initial solitary wave profile and horizontal velocities were allocated. The fluid density ρ and kinematic viscosity ν were 1000 kg/m^3 and $10^{-6} \text{ m}^2/\text{s}$, respectively.

In Figure 4, the computed values of run-up on the slope with $\alpha = 45^\circ$ and the empirical results (Eq. (24)) are compared. The good agreement between the computational results and experimental data shows the ability of the present model to simulate non-breaking solitary wave run-up. Particle configurations for the case of $a = 0.08 \text{ m}$, $d = 0.2 \text{ m}$ at time $t = 0.8 \text{ s}$ are demonstrated in Figure 5 for propagation of a non-breaking wave towards the slope. Due to the steep slope, wave breaking did not occur.

Table 2. Wave parameters and seawall configuration and number of particles in ISPH computations

Test No.	a (m)	d (m)	a/d	Breakwater slope	Number of particles
1	0.04	0.4	0.1	1:1	4619
2	0.06	0.4	0.15	1:1	4789
3	0.08	0.4	0.2	1:1	4959
4	0.06	0.2	0.3	1:1	2899
5	0.08	0.2	0.4	1:1	3059
6	0.04	0.4	0.1	2:1	4414
7	0.06	0.4	0.15	2:1	4564
8	0.08	0.4	0.2	2:1	4714
9	0.06	0.2	0.3	2:1	2564
10	0.08	0.2	0.4	2:1	2714
11	0.04	0.4	0.1	4:1	3977
12	0.06	0.4	0.15	4:1	4127
13	0.08	0.4	0.2	4:1	4277
14	0.04	0.4	0.1	8:1	3935
15	0.06	0.4	0.15	8:1	4085
16	0.08	0.4	0.2	8:1	4235
17	0.04	0.4	0.1	vertical	3883
18	0.06	0.4	0.15	vertical	4033
19	0.08	0.4	0.2	vertical	4183
20	0.06	0.2	0.3	vertical	2447
21	0.08	0.2	0.4	vertical	2597

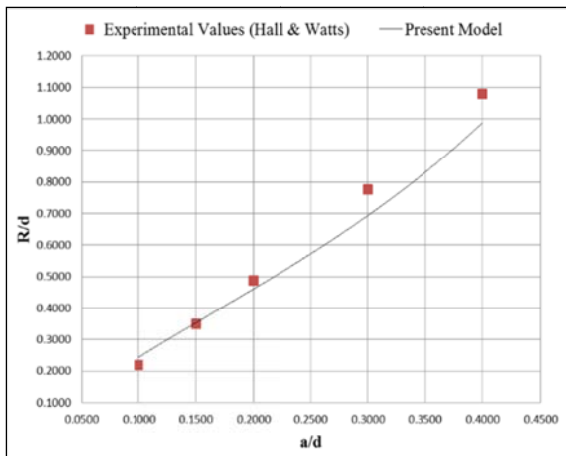


Fig. 4: Comparison between solitary wave run-ups on a slope with $\alpha = 45^\circ$ computed by ISPH model and experimental based formula

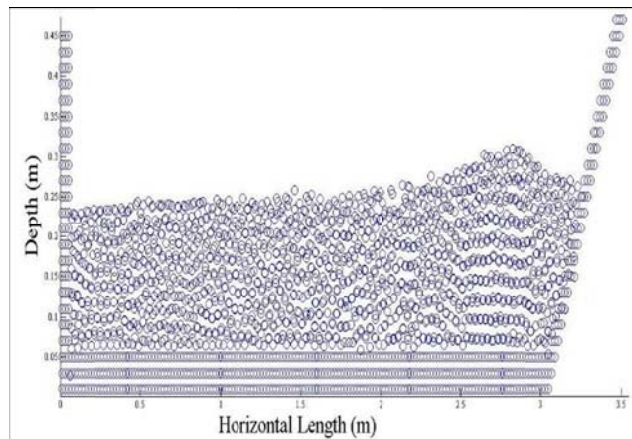


Fig. 5: Particle configurations at $t = 0.8 \text{ s}$ for solitary wave run-up problem simulated by ISPH model

According to the results, solitary wave run-up on other beaches with different slopes (1:1, 2:1, 4:1, 8:1 and vertical slope) were modeled and Results are illustrated in Figure 6. Finally, based on case study results, the formula for solitary wave run-up rate on steep slopes which was second order polynomial was obtained (Eq. 25):

$$R/d = 2.95(a/d)^2 + 1.11(a/d) + 0.05 \quad (25)$$

As can be found in Figure 5, the rate of non-breaking solitary wave run-up on steep slopes was considerably dependant on water depth and wave amplitude rather than slope of beach.

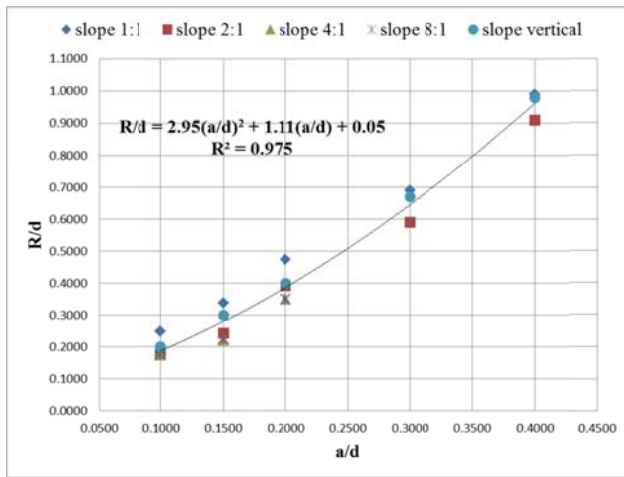


Fig. 6: Equation of solitary wave run-up rate by various amplitude against steep slopes

6. Conclusion

An ISPH flow model developed to simulate water waves. SPH was a meshless method based on particles, which was capable of high accurate modeling of free surface flows with large deformations. In the present model, a new technique was applied to allocate density of the particles for the calculations. By employing this technique, ISPH model was stabilized. The ISPH model was validated by modeling solitary wave propagation on the constant water depth and run-up of non-breaking waves problems. For all of the tests, a satisfactory agreement with the theoretical and experimental results was found. The model application to the non-breaking wave run-up on steep slopes disclosed that the rate of solitary wave run-up was

more sensitive to selection of the water depth and wave amplitude than slope of beaches. The computations of ISPH model by using different particle sizes have found that the convergence and accuracy of the numerical results depended highly on the selected particle spacing and convergence rate of the ISPH model for simulating of water waves was around $O(dr^{18})$.

References

- Ataie-Ashtiani, B., Shobeiry, G. and Farhadi, L., 2008. Modified Incompressible SPH method for simulating free surface problems. *Fluid Dynamic Research*. 40: 637-661.
- Camfield, F.E. and Street, R.L., 1969. Shoaling of solitary waves on small slopes. *Journal of Waterway, Port, Coastal, and Ocean Engineering*. 95: 1-22.
- Chorin, A.J., 1968. Numerical solution of the Navier-Stokes equations. *Mathematics of Computation*. 22: 745-762.
- Cummins, S.J. and Rudman, M., 1999. An SPH projection method. *Journal of Computational Physics*. 152: 584-607.
- Fuhrman, D.R. and Madsen, P.A., 2008. Simulation of nonlinear wave run-up with a high-order Boussinesq model. *Coastal Engineering*, 55: 139-154.
- Hall, J.V. and Watts, J.W., 1953. Laboratory investigation of the vertical rise of solitary waves on impermeable slopes. Technical Memorandum 33, Beach Erosion Board, Office of the Chief of Engineers, U.S. Army Corps of Engineers. 12 P.
- Harlow, F. and Welch, J., 1965. Numerical calculation of time-dependent viscous incompressible flow of fluid with free surface. *The physics of fluids*. 8: 2182-2189.
- Heinter, K.L. and Housner, G.W., 1970. Numerical model for tsunami run-up. *Journal of Waterway, Port, Coastal, and Ocean Engineering*. 3: 701-719.
- Hirt, C.W. and Nichols, B.D., 1981. Volume of Fluid (VOF) Method for the Dynamics of Free

- Boundaries. *Journal of Computational Physics*. 39: 201-225.
- Hsiao, S., Hsu, T., Lin, T. and Chang, Y., 2008. On the evolution and run-up of breaking solitary waves on a mild sloping beach. *Coastal Engineering*. 55: 975-988.
- Kim, S.K., Liu, P.L-F. and Liggett, J.A., 1983. Boundary integral equation solutions for solitary wave generation propagation and run-up. *Coastal Engineering*. 7: 299-317.
- Lee, J.J. and Raichlen, F., 1982. Measurement of velocities in solitary waves. *Journal of Waterway, Port, Coastal, and Ocean Engineering*. 108: 200-218.
- Lo, E.Y.M. and Shao, S., 2002. Simulation of near-shore solitary wave mechanics by an incompressible SPH method. *Applied Ocean Research*. 24: 275-286.
- Lucy, L.B., 1977. A numerical approach to the testing of the fission hypothesis. *Astronomical Journal*, 82: 1013-1024.
- Monaghan, J.J., 1992. Smoothed particle hydrodynamics. *Annual Review of Astronomy and Astrophysics*. 30: 543-574.
- Monaghan, J.J., 1994. Simulating free surface flows with SPH. *Journal of Computational Physics*. 110: 399-406.
- Monaghan, J.J., 1996. Gravity currents and solitary waves. *Physica D: Nonlinear Phenomena*. 98: 523-533.
- Monaghan, J.J. and Kos, A., 1999. Solitary waves on a Cretan beach. *Journal of Waterway, Port, Coastal, and Ocean Engineering*. 125: 145-154.
- Quinlan, N.J., Basa, M. and Lastiwka, M., 2006. Truncation error in mesh-free particle methods. *International Journal for Numerical Methods in Engineering*. 66: 2064-2085.
- Saeki, H., Hanayasu, S., Ozaki, A. and Takagi, k., 1971. The shoaling and run-up height of the solitary wave. *Coastal Engineering Journal*. 14: 25-42.
- Shao, S., 2010. Incompressible SPH flow model for wave interactions with porous media. *Coastal Engineering Journal*. 57: 304-316.
- Shao, S. and Lo, E., 2003. Incompressible SPH method for simulating Newtonian and non-Newtonian flows with a free surface. *Advances in Water Resources*. 26: 787-800.
- Synolakis, C.E., 1986. The running of solitary waves. PhD Thesis, California Institute of Technology, Pasadena, CA. 220 P.
- Vaughan, G.L., Healy, T.R., Bryan, K.R., Sneyd, A.D. and Gorman, R.M., 2008. Completeness conservation and error in SPH for fluids. *International Journal for Numerical Methods in Fluids*. 56: 37-62.
- Wood, D. J., Pedersen, G. K. and Jensen, A., 2003. Modeling of run-up of steep non-breaking waves. *Ocean Engineering*. 30: 625-644.
- Xu, R., Stansby, P.K. and Laurence, D., 2009. Accuracy and Stability in Incompressible SPH (ISPH) Based on the projection method and a new approach. *Journal of Computational Physics*. 228: 6703-6725.
- Zelt, J.A., 1991. The run-up of nonbreaking and breaking solitary waves. *Coastal Engineering*. 15: 205-246.